FULL PAPER

Dalton
www.rsc.org/dalton

Mixed-ligand ytterbium(III) complexes incorporating one or two bidentate (*N*,*O*) amide ligands

Glen B. Deacon,* Craig M. Forsyth and Natalie M. Scott
School of Chemistry, Monash University, Victoria 3800, Australia.
E-mail: glen.deacon@sci.monash.edu.au

Received 3rd April 2003, Accepted 20th June 2003
First published as an Advance Article on the web 7th July 2003

Examples of the ability of the donor-functionalised amide ligands *N*-(2-methoxyphenyl)-*N*-(trimethylsilyl)amide (L^1) and *N*-(2-phenoxyphenyl)-*N*-(trimethylsilyl)amide (L^2) to support mixed-ligand lanthanoid complexes of the type $[Ln(L)_2A]$ or [Ln(L)AB] are described. Reaction of $[Yb(OAr)_3]$ (Ar = $C_6H_3Bu^t_2$-2,6) with two equivalents of $[Li(L^2)]_n$ in hexane gave hexane-soluble, monomeric and five-coordinate $[Yb(L^2)_2(OAr)]$ (**1**) in high yield. Attempted preparation of an analogous $[Yb(L^1)_2(MeCp)]$ complex by reaction of $[Yb(MeCp)Cl_2(thf)]$ with $[Li(L^1)(OEt_2)]_2$ (with a Yb : Li ratio of 1 : 2) in thf instead gave the known $[Yb(L^1)_2(\mu\text{-}Cl)]_2$ (**2**). In contrast, the stable complexes $[Yb(MeCp)(L^1)(\mu\text{-}Cl)]_2$ (**3**) and $[Yb(MeCp)(L^2)(\mu\text{-}Cl)]_2$ (**4**) were readily obtained from 1 : 1 (Li : Yb) reaction of $[Yb(MeCp)Cl_2(thf)]$ with $[Li(L^1)(OEt_2)]_2$ or $[Li(L^2)(dme)]$ in thf. The complexes **1**, **3** and **4** have been characterised by X-ray structure determination.

Introduction

The dramatic catalytic properties of group 3 and lanthanoid metallocenes $[Ln(Cp)_2R]$[1,2] has prompted a search for alternative ancillary ligands that may further exploit new reactivity prospects for these metals.[3,4] Promising results have been achieved for bidentate diorganoamides, such as amidinates,[5–7] ketiminates,[8,9] guanidinates,[10–14] aminotroponimates[15,16] and aminopyridinates,[17,18] as spectator groups for lanthanoid catalysis.[19] We have recently introduced to lanthanoid chemistry some new amide ligands based on an *ortho*-disubstituted phenylene backbone (Fig. 1).[20,21] These have a pendant donor arm, thus chelating to the lanthanoid cation in an 'edge-on' binding mode (Fig. 1, **A**), in contrast to the 'face-on' coordination of Cp (Fig. 1, **B**), the latter giving rise to the characteristic reactivity wedge in metallocene catalysts.[1,2] The bulky substituents on the amide ligand periphery provide steric protection, enabling isolation of heterolepetic lanthanoid(III) complexes of the type $[Ln(L)_2(X)]_2$ (*e.g.* X = Cl, OMe)[21,22] and $[Ln(L)_2(OPh)(thf)]$.[22] In order to further explore the potential of the new L^1 and L^2 ligand systems, we have investigated generation of solvent-free species that incorporate either two 'L' ligands {*e.g.* $[Ln(L)_2A]$-type complexes} or complexes having three disparate ligands {*e.g.* [Ln(L)AB]-type complexes}. We now report the synthesis and structural characterisation of examples of both classes of complex, *viz.* monomeric $[Yb(L^2)_2(OAr)]$ (Ar = $C_6H_3Bu^t_2$-2,6) and dimeric $[Yb(MeCp)(L)(\mu\text{-}Cl)]_2$ (L = L^1, L^2). These complexes demonstrate a wider applicability for the current chelating amide ligands.

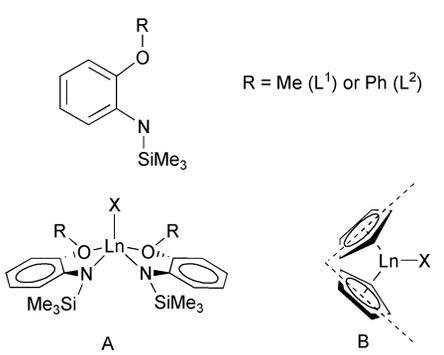

Fig. 1 Structures of L^1 and L^2, and 'edge-on' and 'face-on' binding modes of amide (**A**) and Cp (**B**) ligands, respectively, in lanthanoid complexes.

Results and discussion

The ligands L^1 and L^2 form a variety of well-defined, hydrocarbon-soluble lithium salts,[21,23] of which dimeric $[Li(L^1)(OEt_2)]_2$ and monomeric $[Li(L^2)(dme)]$ are the most suitable for situations where isolated reactants are needed. Strict stoichiometric conditions are generally required for the preparation of the target mixed-ligand complexes free from contamination by homoleptic $[Ln(L)_3]$. We have previously isolated the solvated mixed-ligand aryloxide complex $[Yb(L^2)_2(OPh)(thf)]$[22] unexpectedly from oxidation of a transient $[Yb^{II}(L^2)_2(solvent)_x]$ species, and considered that use of a bulkier OAr group (*e.g.* Ar = $C_6H_3Bu^t_2$-2,6) might yield a solvent-free derivative. Accordingly, reaction of solvent-free $[Li(L^2)]_n$[23] with $[Yb(OAr)_3]$ in a 2 : 1 molar ratio in hexane (Scheme 1) successfully afforded hexane-soluble $[Yb(L^2)_2(OAr)]$ (**1**) in high yield, the eliminated LiOAr having low solubility in this medium.[24]

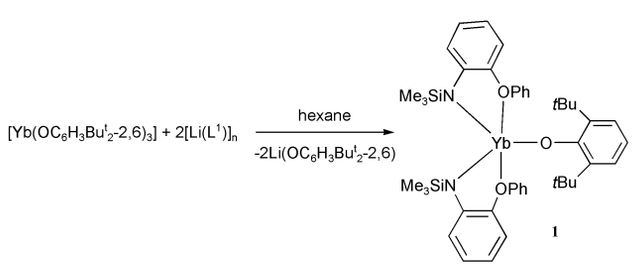

Scheme 1

Complex **1** gave satisfactory elemental analyses (C, H, N) and the infrared spectrum showed the presence of bands attributable to L^2 {by comparison with that of the related $[Nd(L^2)_3]$[21]}, as well as additional strong absorptions at 1411, 845, 801 and 755 cm^{-1}. The last may be a γ(CH) vibration of the 2,6-di-*tert*-butylphenolate ring with three adjacent hydrogens and is observed in the spectra of $[Ln(OAr)_2(s)]$ (s = thf or Et_2O).[25,26] An X-ray crystallographic study revealed that **1** is a monomeric five-coordinate complex comprising a central ytterbium atom surrounded by an oxygen-bound aryloxide group and two chelating L^2 ligands. There are two monomers in the asymmetric unit (one of which is depicted in Fig. 2), but both have a similar structure, the major difference being derived from rotation of one of the Bu^t groups from an eclipsed (Fig. 2) to a staggered arrangement. The ytterbium coordination geometry differs from the idealised square-based pyramid shown in Fig. 1

DOI: 10.1039/b303724j

Table 1 Ytterbium environment in $[Yb(L^2)_2(OAr)]$ (**1**)

Bond distances/Å	
Yb(1)–N(1)	2.068(2)
Yb(1)–N(2)	2.215(3)
Yb(1)–O(1)	2.373(2)
Yb(1)–O(2)	2.363(2)
Yb(1)–O(3)	2.068(2)
Bond angles/°	
N(1)–Yb(1)–N(2)	111.62(9)
N(1)–Yb(1)–O(1)	71.97(8)
N(1)–Yb(1)–O(2)	109.05(8)
N(1)–Yb(1)–O(3)	124.14(9)
N(2)–Yb(1)–O(1)	107.35(8)
N(2)–Yb(1)–O(2)	71.51(8)
N(2)–Yb(1)–O(3)	124.22(9)
O(1)–Yb(1)–O(2)	178.66(7)
O(1)–Yb(1)–O(3)	89.61(8)
O(2)–Yb(1)–O(3)	90.49(8)

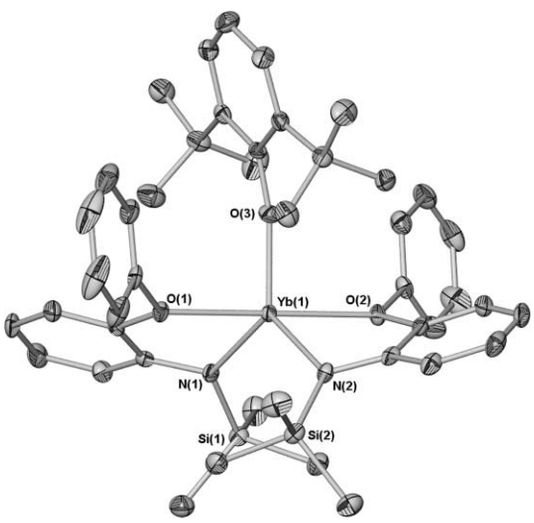

Fig. 2 Structure of one of the independent molecules of **1** with 50% thermal ellipsoids. Hydrogen atoms are omitted for clarity.

(and approaches a trigonal bipyramid) due to a relative twisting of the two L^2 arene backbones by 50.2(2)°. Thus, the two $NSiMe_3$ groups project below the ytterbium atom, whilst the phenyl substituents protrude above, with a resultant near-linear O–Yb–O angle (Table 1). The aryloxide ligand fits neatly into the remaining space; the flat face of the arene ring is flanked by the two OPh groups, whilst the bulky Bu^t substituents are positioned directly above the $NSiMe_3$ groups (Fig. 2). This comfortable accommodation of the bulky OAr ligand by the $Yb(L^2)_2$ environment is reflected in the relatively short Yb(1)–O(3) distance (Table 1) in comparison with $[Ln(OAr)_3(thf)]$[27] and $[Ln(OAr)_2(s)_x]$ (s = thf or Et_2O)[25,26,28] complexes. After corrections for differences in the ionic radii,[29] the subtraction value for **1** of 1.16 Å is short compared with the usual range of 1.22–1.34 Å. This effect appears typical of mixed-ligand lanthanoid aryloxides, *e.g.* $[Sm(C_5Me_5)_2(OAr)]$ (subtraction value 1.12 Å)[30] or $[YbCl_2(OAr)(thf)_3]$ (1.22 Å),[31] and presumably the $[Ln(OAr)_3(thf)]$ or $[Ln(OAr)_2(s)_x]$ complexes suffer from significant ligand–ligand repulsions as a consequence of the presence of at least four Bu^t groups. The $Yb(L^2)_2$ arrangement in **1** also differs markedly from that of six-coordinate $[Yb(L^2)_2(OPh)(thf)]$, with the ytterbium atom and the two L^2 ligands more in a plane in **1** rather than being almost perpendicular, as they are in the latter. This variation contrasts with the almost unchanging $Ln(Cp)_2$ structural fragment in metallocene systems.

To provide a counterpoint to the mixed-ligand aryloxide complex **1**, we attempted to prepare an analogous $[Ln(L)_2A]$ species, where A is a polyhapto-cyclopentadienyl ligand, utilising an alternative synthetic strategy, *viz*. metathesis from a $[Yb(Cp)X_2]$ (X = halide) species. However, reaction of $[Yb(MeCp)Cl_2(thf)]$ with $[Li(L^1)(OEt_2)]_2$ in a Li : Ln ratio of 2 : 1 in thf unexpectedly afforded the known mixed-ligand bis(amido) chloride complex $[Yb(L^1)_2(\mu\text{-}Cl)]_2$ (**2**)[21] in high yield [Scheme 2(i)]. Previously, an attempt to prepare an analogous target complex, $[Yb(L^1)_2(Cp)]$, by an oxidation reaction from $[Yb(L^1)_2(s)_x]$ also failed and gave a rearranged product, $[Yb(Cp)_2(L^1)]$.[20] Considering the structures of the two aryloxide complexes **1** and $[Yb(L^2)_2(OPh)(thf)]$, the $Yb(L)_2$ unit appears to accommodate the increase in coordination number in the latter by compression of the OPh substituents of the amide ligands into a *cis* array around the more saturated metal. Presumably, the extra coordination site required by a 'face-on' Cp ligand destabilises the resulting $[Yb(L)_2(Cp)]$ complex by requiring closer compression of these groups preventing its isolation.

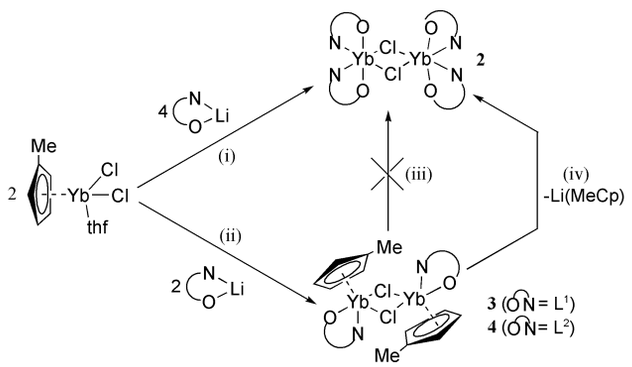

Scheme 2 (i) 2 $[Li(L^1)(OEt_2)]_2$, thf; crystallisation from hexane. (ii) $[Li(L^1)(OEt_2)]_2$ or 2 $[Li(L^2)(dme)]$, thf; crystallisation from hexane. (iii) $2Yb(MeCp)(L^1)Cl$ (**3**) $\not\rightarrow$ $Yb(MeCp)_2Cl + Yb(L^1)_2Cl$ (**2**); rearrangement does not occur. (iv) $[Li(L^1)(OEt_2)]_2$, hexane; Li(MeCp) removed by filtration.

In contrast to the above reaction, treatment of $[Yb(MeCp)Cl_2(thf)]$ with $[Li(L^1)_2(OEt_2)]_2$[21] or $[Li(L^2)(dme)]$[23] in a 1 : 1 (Li : Ln) ratio in thf afforded examples of the second type of target mixed-ligand complexes, $[Yb(MeCp)(L^1)(\mu\text{-}Cl)]_2$ (**3**) and $[Yb(MeCp)(L^2)(\mu\text{-}Cl)]_2$ (**4**), respectively [Scheme 2(ii)]. The successful isolation of **3** and the high yield (74%) of **2** from the 2 : 1 (Li : Ln) reaction excludes a possible **3** $\longrightarrow$ **2** rearrangement [Scheme 2(iii); maximum possible yield 50%] as the source of the latter from the 2 : 1 reaction. Thus, in the formation of **2**, the initial product is presumably **3**, which subsequently eliminates insoluble LiMeCp in hexane. This scenario was independently confirmed by a small scale reaction of isolated **3** with $[Li(L^1)(OEt_2)]_2$ in a 1 : 1 (Li : Yb) ratio in hexane, which gave **2** and Li(MeCp) in moderate yield [Scheme 2(iv)].

The compositions of **3** and **4** were established by elemental analyses (C, H, N) and the presence of trivalent ytterbium was confirmed by the observation of characteristic[32] f $\longleftarrow$ f transitions around 1000 nm in the near infrared spectrum. A ligand-to-metal charge transfer (from both MeCp and L^1/L^2) absorption in the visible region at 426 (**3**) and 428 nm (**4**) accounts for the intense red colour of the complexes. The IR spectra show strong absorptions characteristic of L^1 and L^2, and obscuring those expected for the MeCp ligand.[33] The mass spectrum of **4** exhibits no peaks for metal-containing ions attributable to dinuclear species, but the mononuclear ion $[Yb(MeCp)(L^2)Cl]^+$ was observed, in addition to the organic fragments $[L^2]^+$ and $[MeCp]^+$.

The single crystal X-ray structures of **3** (Fig. 3) and **4** (Fig. 4) were determined. The ytterbium coordination environments are virtually the same, despite the greater steric demand of L^2 compared with L^1. Selected bond lengths and angles are listed in Tables 2 and 3. The asymmetric unit of each structure comprises half of a dimeric $[Yb(MeCp)(L)(\mu\text{-}Cl)]_2$ unit, bridged by two chloride atoms, the other half related by

Table 2 Selected bond distances (Å) in $[Yb(MeCp)(L)(\mu\text{-}Cl)]_2$ {L = L^1 (**3**), L^2 (**4**)}

	3	**4**
Yb(1)–N(1)	2.207(3)	2.205(2)
Yb(1)–O(1)	2.337(3)	2.359(2)
Yb(1)–Cl(1)	2.646(1)	2.641(1)
Yb(1)–Cl(1A)[a]	2.655(1)	2.647(1)
Yb(1)–C(1C)[b]	2.307	2.301
Yb(1)–C(1)	2.637(4)	2.631(3)
Yb(1)–C(2)	2.587(4)	2.609(3)
Yb(1)–C(3)	2.564(5)	2.586(3)
Yb(1)–C(4)	2.597(4)	2.565(3)
Yb(1)–C(5)	2.624(4)	2.588(3)

[a] Symmetry transformations used to generate equivalent atoms: $-x+2, -y+2, -z+1$ (**3**); $-x+1, -y, -z$ (**4**). [b] C(1C) = centroid of C(1)–C(5).

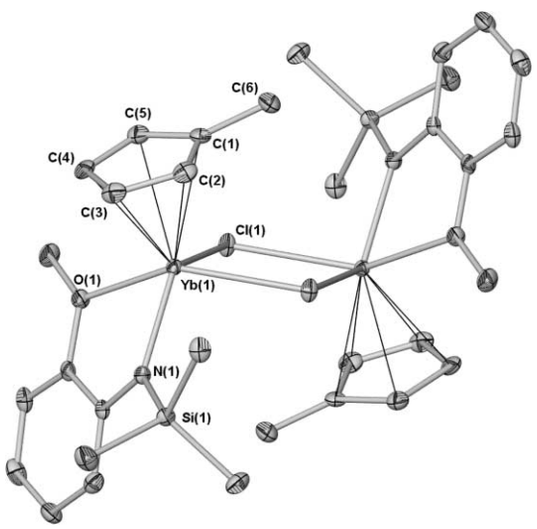

Fig. 3 Molecular structure of **3** with 50% thermal ellipsoids. Hydrogen atoms are omitted for clarity.

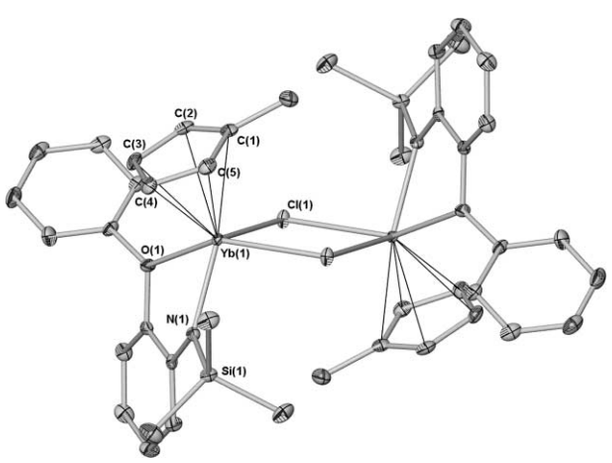

Fig. 4 Molecular structure of **4** with 50% thermal ellipsoids. Hydrogen atoms are omitted for clarity.

inversion, generating a planar Yb_2Cl_2 core. Thus, pairs of MeCp, OR and $N(SiMe_3)$ groups have a *transoid* disposition across the Yb_2Cl_2 bridge. The unique metal environment in each complex is a seven-coordinate pseudo-square-based pyramid, with the centroid of the η^5-methylcyclopentadienyl ligand occupying the apical position. These two structures clearly show the contrasting coordination modes of the MeCp ('face-on') and L^1 and L^2 ('edge-on') ligands. Considering the structures of the series of complexes $[Ln(L^1)_2(\mu\text{-}Cl)]_2$ (**2**),[21] $[Yb(MeCp)(L)(\mu\text{-}Cl)]_2$ {L = L^1 (**3**), L^2 (**4**)} and $[Yb(MeCp)_2(\mu\text{-}Cl)]_2$ (**5**),[34] and denoting the amide nitrogens or the centroids

Table 3 Comparison of ytterbium geometries (°) in $[Yb(L^1)_2(\mu\text{-}Cl)]_2$ (**2**), $[Yb(MeCp)(L)(\mu\text{-}Cl)]_2$ {L = L^1 (**3**), L^2 (**4**)} and $[Yb(MeCp)_2(\mu\text{-}Cl)]_2$ (**5**)

	2[21]	**3**	**4**	**5**[34]
A–Yb–A[a]	113.5(3), 112.7(3)	130.9	130.4	126.7
A–Yb–Cl	151.2(2), 152.3(2)	117.47(11)	114.29(6)	112.4
	144.3(2), 143.3(2)	94.19(11)	92.33(6)	109.4
	91.0(2), 93.8(2)	109.4	114.1	109.1
	88.5(2), 86.7(2)	108.1	107.4	108.0
Cl–Yb–Cl	79.55(7), 79.47(7)	79.60(5)	78.51(2)	82.05(5)
Yb–Cl–Yb	98.72(8), 99.12(8)	100.04(5)	101.49(2)	97.95(5)

[a] A denotes N in **2**, N or centroid of C(1)–C(5) in **3** and **4**, and centroid of C(1)–C(5) or centroid of C(7)–C(11) in **5**.

of the MeCp rings as 'A', there is an intriguing similarity in the geometry of **3**, **4** and **5**, which show comparable A–Yb–A and A–Yb–Cl angles (Table 3). In contrast, **2** has narrower A–Yb–A angles and some considerably more *transoid* A–Yb–Cl angles (Table 3). These geometrical differences between **2**, and **3**, **4** and **5** appear to be reflected in the bond distance patterns of the three complexes. Thus, values derived by subtraction of the Yb^{3+} ionic radius from the Yb–N and Yb–O distances in **3** (1.28 and 1.40 Å, respectively) and **4** (1.28 and 1.43 Å, respectively) indicate shorter bonds than found for the respective heteroleptic chlorides **2** (1.32 and 1.48 Å, respectively) and $[Nd(L^2)_2(\mu\text{–}Cl)]_2\cdot 2PhMe$ (1.33 and 1.56 Å, respectively).[21] Similarly, an evaluation of the metal–chloride distances in **3** (1.72 Å) and **4** (1.71 Å) shows these bonds are also significantly shorter than in **2** (1.81 Å) and $[Nd(L^2)_2(\mu\text{-}Cl)]_2.(PhMe)_2$ (1.84 Å),[21] but are only marginally longer than those of **5** (1.66 Å).[34] Thus, the bonding patterns of **3** and **4** are more consistent with a bis-(cyclopentadienyl) rather than a bis(amido) ligand set. Overall, the Yb–N, Yb–O, and Yb–Cl bond distances in **3** and **4** are comparable to those found in the linked cyclopentadienyl-amide complex $[Y(\eta^5\text{:}\eta^1\text{-}SiMe_2C_5Me_4NCMe_2Et)(thf)(\mu\text{-}Cl)]_2$ (subtraction values Y–N 1.28, Y–O 1.45, Y–Cl 1.67 Å),[35] which parallels (**3**) and (**4**), with the coordinated thf occupying a similar position to that of the ether substituent on L^1 and L^2.

Conclusions

Novel, solvent-free, ytterbium(III) complexes were prepared *via* metathesis reactions, showing that the amide ligands L^1 and L^2 can support a variety of mixed-ligand lanthanoid environments. Unusually low coordination number (<6) complexes, *e.g.* five-coordinate $[Yb(L^2)_2(OAr)]$, are also accessible. Whilst compositionally similar to the many $[Ln(Cp)_2A]$ compounds and the more limited [Ln(Cp)AB] complexes in terms of solvent coordination and structural types (*e.g.* monomer *vs.* dimer), the 'edge-on' binding of the bidentate-amide ligands provides subtle structural differences which may be exploitable as catalytic ancillaries. The range of amido-lanthanoid complex types now available with the present ligands include both $[Ln(L)_2A]$ and [Ln(L)(Cp)A], analogous to $[Ln(Cp)_2A]$ and [Ln(Cp-NR)A] (Cp-NR = *ansa*-cyclopentadienyl-amide ligand), both of which are active catalytic precursors.[2,36]

Experimental

All reactions were carried out under dry nitrogen using a dry box and standard Schlenk techniques. Solvents were dried by distillation from sodium wire–benzophenone. IR spectra (4000–650cm^{-1}) were recorded from Nujol mulls sandwiched between NaCl plates with a Perkin Elmer 1600 FTIR spectrometer. Mass spectra were recorded using a VG Trio-1 GC mass spectrometer. Each listed *m*/*z* value for metal-containing ions is the most intense peak of a particular cluster pattern, in good agreement with the calculated pattern. Elemental analyses

Table 4 Crystal and refinement data

Compound	$[Yb(L^2)_2(OAr)]$ (**1**)	$[Yb(MeCp)(L^1)(\mu\text{-}Cl)]_2$ (**3**)	$[Yb(MeCp)(L^2)(\mu\text{-}Cl)]_2$ (**4**)
Formula	$C_{44}H_{57}N_2O_3Si_2Yb$	$C_{16}H_{23}ClNOSiYb$	$C_{21}H_{25}ClNOSiYb$
M	891.14	481.93	544.00
a/Å	13.8480(1)	8.5538(3)	9.6568(1)
b/Å	15.6657(2)	9.7537(2)	8.7267(1)
c/Å	20.1433(2)	12.0433(2)	25.3241(3)
α/°	70.702(1)	76.953(1)	90
β/°	82.812(1)	78.027(1)	98.997(1)
γ/°	88.253(1)	64.868(1)	90
V/Å^3	4233.3(15)	879.1(3)	2107.9(7)
Crystal system	Triclinic	Triclinic	Monoclinic
Space group	$P\bar{1}$	$P\bar{1}$	$P2_1/c$
Z	4	2	4
ρ_{calcd}/g cm^{-1}	1.398	1.821	1.714
μ(Mo-K$_\alpha$)/mm^{-1}	2.305	5.537	4.630
$2\vartheta_{max}$/°	56.6	56.6	56.6
N, N_o	19743, 15003	4293, 3835	5202, 4877
R, R_w (observed data)	0.0316, 0.0551	0.0322, 0.0711	0.0213, 0.0500
R, R_w (all data)	0.0581, 0.0653	0.0394, 0.0735	0.0239, 0.0511

(C, H, N) were determined by the Campbell Microanalytical Service, University of Otago, New Zealand. Metal analyses were carried out by complexiometric titration with Na_2EDTA.[37,38] The following reagents were prepared according to the reported methods: $[Li(L^1)_2(OEt_2)]_2$,[21] $[Li(L^2)(dme)]$,[23] $[Li(L^2)]_n$;[23] $[Yb(OC_6H_3Bu^t_2\text{-}2,6)_3]$ was prepared analogously to the Sc, Y, La and Sm derivatives.[39]

$[Yb(L^2)_2(OC_6H_3Bu^t_2\text{-}2,6)]$ (1)

Tris(2,6-di-*tert*-butylphenolato)ytterbium(III) (0.090 g, 0.11 mmol), $[Li(L^2)]_n$ (0.060 g, 0.22 mmol) and hexane (20 cm^3) were added to a flask, and the mixture was stirred for 15 h. The red reaction mixture was cooled to −78 °C, affording a white precipitate. The mixture was filtered and the filtrate allowed to warm to room temperature. After evaporation to low volume and standing for 2 h, orange crystals (suitable for X-ray analysis) of the title complex formed (0.070 g, 73%). (Found: C, 59.0; H, 6.8; N, 2.9; $C_{44}H_{57}N_2O_3Si_2Yb$ requires C, 59.3; H, 6.5; N, 3.1%.) IR (Nujol) ν/cm^{-1}: 1594 s, 1558 w, 1478 s, 1411 vs, 1351 w, 1280 vs, 1244 s, 1183 s, 1158 s, 1098 vs, 1074 w, 1048 br m, 1022 w, 1004 w, 916 vs, 861 s, 845 s, 827 s, 801 vs, 755 s, 734 s, 693 vs, 680 w, 659 m, 628 w, 593 w.

Synthesis and characterisation of $[Yb(MeCp)Cl_2(thf)]$

The compound $[Yb(MeCp)Cl_2(thf)]$ was prepared in a metathesis reaction similar to the synthesis of $[Er(C_5H_5)Cl_2(thf)_3]$.[40] To solid $YbCl_3(thf)_3$ (1.05 g, 2.11 mmol) and Tl(MeCp) (0.60 g, 2.11 mmol) was added thf, and the reaction mixture was stirred at room temperature for 12 h. Filtration and evaporation to dryness yielded a dark red material (0.52 g, 62%). (Found: C, 29.0; H, 5.0; $C_{10}H_{15}Cl_2OYb$ requires C, 30.4; H, 3.8%.) IR (Nujol) ν/cm^{-1}: 1299 w, 1170 w, 1074 w, 1013 s, 921 m, 863 br s, 771 w, 722 s, 668 w.

Reaction of $[Yb(MeCp)Cl_2(thf)]$ with $[Li(L^1)(OEt_2)]_2$ (Li : Yb molar ratio of 2 : 1)

To solid $[Li(L^1)(OEt_2)]_2$ (0.29 g, 0.50 mmol) and $[Yb(MeCp)Cl_2(thf)]$ (0.28 g, 0.50 mmol) was added thf (40 cm^3). The resulting dark red mixture was stirred for 12 h at room temperature, the solvent was removed under vacuum and hexane was added (30 cm^3). The mixture was filtered and the red filtrate concentrated to *ca.* 15 cm^3 to yield large red crystals of (by IR) **2** (0.22 g, 74%). Unit cell data—$C_{40}H_{64}Cl_2N_4O_4Si_4Yb_2$, M = 1194.3, monoclinic, a = 14.614(1), b = 18.063(1), c = 19.012(1) Å; α = 90, β = 92.44, γ = 90°; V = 5015 Å^3, $T \approx$ 123 K—are in agreement with those reported previously.[21]

$[Yb(MeCp)(L^1)(\mu\text{-}Cl)]_2$ (3)

To a thf solution (40 cm^3) of $[Yb(MeCp)Cl_2(thf)]$ (0.20 g, 0.50 mmol) was added $[Li(L^1)(OEt_2)]_2$ (0.14 g, 0.25 mmol). After stirring for 12 h, the solvent was removed under reduced pressure and hexane (30 cm^3) was added, giving a white precipitate. The red solution was filtered and the filtrate volume reduced to 15 cm^3 under vacuum. The dark red/green dichroic crystals of the title compound formed on standing for 2 weeks (0.17 g, 72%). (Found: C, 39.7; H, 4.7; N, 3.0; $C_{32}H_{46}Cl_2N_2O_2Si_2Yb_2$ requires C, 39.9; H, 4.8; N, 2.9%) IR (Nujol) ν/cm^{-1}: 1594 s, 1560 w, 1486 s, 1320 w, 1283 vs, 1247 vs, 1238 s, 1214 m, 1164 vs, 1119 vs, 1068 w, 1052 m, 1032 m 1011s, 911 vs, 897 w, 827 vs, 790 w, 768 vs, 746 w, 732 vs, 678 s, 629 s, 599 w. Vis-near IR (DME) λ_{max}/nm (ε/dm^3 mol^{-1} cm^{-1}): 426 (230), 938 (4), 982 (42), 994 (18).

$[Yb(MeCp)(L^2)(\mu\text{-}Cl)]_2$ (4)

To solid $[Yb(MeCp)Cl_2(thf)]$ (0.27 g, 0.72 mmol) and $[Li(L^2)(dme)]$ (0.26 g, 0.72 mmol) was added thf (40 cm^3), and the mixture was stirred for 12 h. The solvent was evaporated to dryness and hexane (30 cm^3) was added giving a white precipitate. The orange solution was filtered and the filtrate volume reduced to 15 cm^3 under vacuum. Dark purple crystals (suitable for X-ray analysis) of the title compound deposited on standing (0.24 g, 62%). (Found: C, 46.1; H, 4.7; N, 2.7; $C_{42}H_{50}Cl_2N_2O_2Si_2Yb_2$ requires C, 46.4; H, 4.6; N, 2.6%) IR (Nujol) ν/cm^{-1}: 1586 s, 1558 w, 1303 w, 1281 vs, 1245 vs, 1183 s, 1157 vs, 1100 vs, 1047 s, 1026 m, 960 w, 908 vs, 850 s, 831 vs, 786 s, 726 m, 695 s, 680 w, 632 w. MS m/z: 509 (20%) $[Yb(L^2)(C_5H_4Me)]^+$, 464 (5) $[Yb(L^2)(C_5H_4Me) - 3Me]^+$, 432 (<1) $[Yb(L^2)(C_5H_4Me) - C_6H_5]^+$, 416 (<1) $[Yb(L^2)(C_5H_4Me) - OC_6H_5]^+$, 337 (5) $[Yb(C_6H_4NSiMe_3)]^+$, 257 (10) $[(L^2H)]^+$, 226 (10) $[(L^2) - 2Me]^+$, 165 (15) $[OC_6H_4NHSiMe_2]^+$, 150 (15) $[C_6H_4ONHSiMe]^+$, 135 (20) $[C_6H_5ONHSi]^+$, 73 (100) $[SiMe_3]^+$, 58 (25) $[SiMe_2]^+$. Vis-near IR (DME) λ_{max}/nm (ε/dm^3 mol^{-1} cm^{-1}): 428 (241), 926 (6), 949 (13), 988 (78), 995 (22).

Reaction of $[Yb(MeCp)(L^1)(\mu\text{-}Cl)]_2$ with $[Li(L^1)(OEt_2)]_2$ (1 : 1 Li : Yb ratio)

Treatment of $[Yb(MeCp)(L^2)(\mu\text{-}Cl)]_2$ (0.10 g, 0.10 mmol) with $[Li(L^1)(OEt_2)]_2$ (0.06 g, 0.10 mmol) in hexane resulted in a white precipitate and a red solution. The reaction mixture was filtered and the filtrate volume reduced, affording red crystals of **2** (0.06 g, 51%). The infrared spectrum was similar to that of the authentic compound.[21]

X-Ray crystallography

Under an inert atmosphere, the air- and moisture-sensitive crystals were covered in viscous oil and mounted onto a glass fibre. Low-temperature (~123 K) data were collected on an Enraf-Nonius CCD area-detector diffractometer (Mo-K$_\alpha$ radiation, λ = 0.7107$_3$ Å; frames comprised of 1.0° increments in ϕ and ω,

yielding a sphere of data) with proprietary software (Nonius B.V., 1998). Each data set was merged (R_{int} as quoted) to N unique reflections; the structures were solved by conventional methods and refined with anisotropic thermal parameter forms for the non-hydrogen atoms by full-matrix least-squares on all F^2 data using the SHELX 97 software package.[41] Hydrogen atoms were included in calculated positions and allowed to ride on the parent carbon atom with isotropic thermal parameters. Data were corrected for absorption by either empirical (**1**, **4**) or numerical (**3**) methods. Crystal data and refinement details for each compound are listed in Table 4.

CCDC reference numbers 207491–207493.

See http://www.rsc.org/suppdata/dt/b3/b303724j/ for crystallographic data in CIF or other electronic format.

Acknowledgements

We are grateful to the Australian Research Council for support and for an Australian Postgraduate Scholarship and a Monash Publications Award to N. M. S.

References

1 H. Yasuda, *J. Organomet. Chem.*, 2002, **647**, 128.
2 G. A. Molander and J. A. C. Romero, *Chem. Rev.*, 2002, **102**, 2161.
3 A. Togni and L. M. Venanzi, *Angew. Chem., Int. Ed. Engl.*, 1994, **33**, 497.
4 R. Kempe, *Angew. Chem., Int. Ed.*, 2000, **39**, 468.
5 Y. J. Luo, Y. M. Yao, Q. Shen, J. Sun and L. H. Weng, *J. Organomet. Chem.*, 2002, **662**, 144.
6 S. Bambirra, A. Meetsma, B. Hessen and J. H. Teuben, *Organometallics*, 2001, **20**, 782.
7 F. T. Edelmann, *Coord. Chem. Rev.*, 1995, **137**, 403.
8 L. Bourget-Merle, M. F. Lappert and J. R. Severn, *Chem. Rev.*, 2002, **102**, 3031.
9 Y. Yao, Y. Zhang, Q. Shen and K. Yu, *Organometallics*, 2002, **21**, 819.
10 Y. J. Luo, Y. M. Yao, Q. Shen, K. B. Yu and L. H. Weng, *Eur. J. Inorg. Chem.*, 2003, 318.
11 Y. J. Luo, Y. M. Yao and Q. Shen, *Macromolecules*, 2002, **35**, 8670.
12 P. J. Bailey and S. Pace, *Coord. Chem. Rev.*, 2001, **214**, 91.
13 G. R. Giesbrecht, G. D. Whitener and J. Arnold, *J. Chem. Soc., Dalton Trans.*, 2001, 923.
14 Z. Lu, G. P. A. Yap and D. S. Richardson, *Organometallics*, 2001, **20**, 706.
15 P. W. Roesky, *Chem. Ber*, 1997, **130**, 859.
16 P. W. Roesky and M. R. Bürgstein, *Inorg. Chem.*, 1999, **38**, 5629.
17 A. Spannerberg, M. Oberthur, H. Noss, A. Tillack, P. Arndt and R. Kempe, *Angew. Chem., Int. Ed.*, 1998, **37**, 2079.
18 A. Spannenberg, P. Arndt and R. Kempe, *Angew. Chem., Int. Ed.*, 1998, **37**, 832.
19 R. Anwander, *Top. Organomet. Chem.*, 1999, **2**, 1.
20 G. B. Deacon, C. M. Forsyth, N. M. Scott, B. W. Skelton and A. H. White, *Aust. J. Chem.*, 2001, **54**, 439.
21 G. B. Deacon, C. M. Forysth and N. M. Scott, *Eur. J. Inorg. Chem.*, 2002, 1425.
22 G. B. Deacon, C. M. Forsyth and N. M. Scott, *Eur. J. Inorg. Chem.*, 2000, 2501.
23 G. B. Deacon, C. M. Forsyth and N. M. Scott, *J. Chem. Soc., Dalton Trans.*, 2001, 2494.
24 P. B. Hitchcock, M. F. Lappert, R. G. Smith, R. A. Bartlett and P. P. Power, *J. Chem. Soc., Chem. Commun.*, 1988, 1007.
25 G. B. Deacon, P. B. Hitchcock, M. F. Lappert, P. MacKinnon and R. H. Newnham, *J. Chem. Soc., Chem. Commun.*, 1989, 935.
26 G. B. Deacon, T. Feng, P. MacKinnon, R. H. Newnham, S. Nickel, B. W. Skelton and A. H. White, *Aust. J. Chem.*, 1993, **46**, 387.
27 G. B. Deacon, T. Feng, S. Nickel, M. I. Ogden and A. H. White, *Aust. J. Chem.*, 1992, **45**, 671.
28 J. R. van den Hende, P. B. Hitchcock, S. A. Holmes, M. F. Lappert, W.-P. Leung, T. C. W. Mak and S. Prasher, *J. Chem. Soc., Dalton Trans.*, 1995, 1427.
29 R. D. Shannon, *Acta. Crystallogr., Sect. A*, 1976, **32**, 751.
30 Z. Hou, Y. Zhang, T. Yoshimura and Y. Wakatsuki, *Organometallics*, 1997, **16**, 2963.
31 Y. Yao, Q. Shen and J. Sun, *Polyhedron*, 1998, **17**, 519.
32 F. Calderazzo, R. Pappalardo and S. Losi, *J. Inorg. Nucl. Chem.*, 1966, **28**, 987.
33 G. B. Deacon, A. J. Koplick and T. D. Tuong, *Aust. J. Chem.*, 1984, **37**, 517 and references therein.
34 E. C. Baker, L. D. Brown and K. N. Raymond, *Inorg. Chem.*, 1975, **14**, 1376.
35 S. Arndt, P. Voth, T. P. Spaniol and J. Okuda, *Organometallics*, 2000, **19**, 4690.
36 Z. Hou and Y. Wakatsuki, *J. Organomet. Chem.*, 2002, **647**, 61.
37 J. L. Atwood, W. E. Hunter, A. L. Wayda and W. J. Evans, *Inorg. Chem.*, 1981, **20**, 4115.
38 G. B. Deacon, T. Feng, C. M. Forsyth, A. Gitlits, D. C. R. Hockless, Q. Shen, B. W. Skelton and A. H. White, *J. Chem. Soc., Dalton Trans.*, 2000, 961.
39 F. T. Edelmann, *Lanthanides and Actinides*, in Herrmann/Brauer, *Synthetic Methods of Oganometallic and Inorganic Chemitry*, ed. W. A. Hermann, Georg Thieme, Stuttgart, 1997.
40 T. J. Marks and R. D. Ernst, *Scandium, Yttrium and the Lanthanides and Actinides*, in *Comprehensive Organometallic Chemistry I*, ed. G. Wilkinson, F. G. A. Stone and E. W. Abel, Pergamon, Oxford, 1982.
41 G. M. Sheldrick, SHELX 97, Program for Crystal Structure Determination, Universität Göttingen, Germany, 1997.